MULTIPHASE FLOW BEHAVIOUR IN VUGULAR CARBONATES USING X-RAY CT

P. Olivier[1], L. Cantegrel[1], J. Laveissière[1], N. Guillonneau[2]
1. Total, France ; 2. Ecole Centrale Lille, France

This paper was prepared for presentation at the International Symposium of the Society of Core Analysts held in Abu Dhabi, UAE, 5-9 October, 2004

ABSTRACT

This paper focuses on the interpretation process to improve unsteady-state flow results when affected by small-scale heterogeneity. Permeability contrasts, materialized by grapes of vugs interbedded in dense carbonate matrix, lead to anomalous relative permeabilities curve shapes which are associated with early water breakthroughs.
Effects of small-scale heterogeneities, flow direction and wettability state are addressed with the use of modern visualization techniques to understand the impact of these features upon waterflooding conventional methods in one vuggy layer.
Two waterflood tests were performed using one carbonate core according to the unsteady-state and steady-state methods. The differential pressure, fluid productions and saturation profiles as a function of time were acquired in both experiments.
CT scanning allows imaging the porosity and permeability distributions while following up the progression of miscible tracer front in a first-contact-miscible flow. Then, these results are used to build-up a 3-D fine-gridded model to match multirate waterflood laboratory tests based on 2 facies -vugs & matrix. In the same manner, this model was run to simulate the steady-state flow. The main conclusions for this study are:

- CT-scan images highlight the water front deformation ahead in the vugs as double porosity mechanism.
- Unsteady state flow interpretation can greatly be improved with 3D fine-gridded model that take into account small scale heterogeneities and provide smooth relative permeabilities for the macropore and micropore systems.
- Imbibition capillary pressure greatly influences the sweep efficiency (water hold-up) and oil production in the case of oil wet systems.

INTRODUCTION

Carbonates rock often display a wide pore size distribution resulting from diagenetic events, especially when material dissolution is occurring. These events bring the system to a double porosity model- matrix and vugs- which are interconnected in a way that the linear displacement behaviour is complex.
To understand the impacts of the small-scale heterogeneities, laboratory studies are essential to predict vuggy carbonates producibility. Incorporating these effects in full-field model may also improve reservoir management and ultimately enhance the oil recovery. Despite careful selection of full-sizes for laboratory corefloods, it is well known that

heterogeneities in core samples can disturb and influence multiphase flow and thus that conventional analysis is likely to be inadequate. On the other hand, reservoir cored samples may sometimes not offer further choice than heterogeneous rocks to cope with.
Several references in the literature illustrate the large impact of the small-scale heterogeneity in the flow stability. Hamon et al [1] pointed out that unsteady-state flow is very sensitive to along-bedding heterogeneity of permeability whereas steady-state flow is more robust when isoperms and flow direction are parallel. Kamal et al [2] used flow visualisation to pinpoint in four distinct carbonates rocks the reduction of the remaining oil saturation through multirate flow tests. They demonstrated that by increasing the pressure gradient upon a specific pore structure, oil throughput is essentially generated from reduction of ROS. Archer et al [3] found that conventional relative permeability interpretation methods (JBN technique) were inadequate for their experiments in vuggy material, leading to anomalous curve shapes associated with water breakthrough ahead of the main flood front. Technology advances in rock characterisation and modern visualisation techniques pave the way for more reliable results on local saturation development. Narayanan et al [4] studied miscible displacement under X-ray CT, in a vugular carbonate sample, and concluded that centimetre-scale heterogeneities control the local brine concentration fluctuations. The overall information in these studies is related to the effects induced by small-scale heterogeneities for multiphase transport through porous media.

In the first part of this paper, two laboratory tests under Unsteady State (USS) and Steady State (SS) imbibitions are presented in one intend of suitability of one technique over the other. For this purpose, both were carried out on the same heterogeneous carbonate rock.
The following part is focused on the visualisation of small-scale heterogeneities arrangement and underline high conductive paths in a first miscible-contact test with a mobility ratio of unity. Also, the construction of a 3D finely gridded (2x2x2 mm) model with its calibration process is presented for the selected carbonate rock.
Eventually, waterflooding interpretations are based on history matching of oil production, differential pressure and incorporating local saturation profiles. Simulations through 1D homogeneous model and then with the 3D model are computed in terms of relative permeabilities and capillary pressures.

EXPERIMENTS

Core Selection

A vugular carbonate core sample was selected according to visual inspection of thin sections, pore-size distribution (mercury injection), mini-permeability map, CTscan and with a miscible tracer test. Description of thin section shows a highly porous grainstone in contact with wackestone bringing a high pore size macropores /micropores contrast (Figure 1). Purcell data (Figure 2) are displayed as a function of pore throat size and reveal a bimodal distribution characterising interplay of macroporosity (vugs) and microporosity (matrix). The cut-off pore throat size between both systems range in 1 to 3 µm. Figure 3 presents a permeability map that accurately captures all the small-scale heterogeneities. An

automated probe permeameter is used along several lines and thus vugs sites can be pinpointed. Table 1 summarizes the core properties and waterflood results.
Tomographic pictures show the evidence of vugs in the core of the Full-size corroborating what was seen on the external surface (Figure 4).
To further characterise this carbonate rock and ascertain its double porosity behaviour, a Brine/Brine tracer test was run (Figure 5). It is an estimate of the level of heterogeneity that highlights the preferential paths only if a sufficient injection is applied avoiding molecular diffusion which is unrepresentative of an immiscible flooding (hydrodynamic dispersion). As compared with homogeneous sample it is visible that effluent dispersion curve pictures an early breakthrough, with a tilted front and a long tail shape.
On one companion plug the oil/water drainage-imbibition capillary curves was measured and the slightly oil-wet sample property was assessed. The imbibition oil/water capillary pressure is entered in the 1D model (Figure 20) and further compared with one history matching Unsteady State flow.

Unsteady State Flow (USS)
The sample was saturated with brine salinity of 150 g/l Eq NaCl and the core water permeability was measured. Initial water saturation was set before to saturate core with toluene and prior to flush it with stock tank oil for wettability restoration. A three weeks ageing period is realised by injecting oil at low flow rate, 2cc/h. Then, lightened stock tank oil (1.0 cp) is used to respect the viscosity ratio between reservoir brine and oil. The density at the outlet core is checked to determine when all non lighted oil is fully replaced. Ultimately, the effective oil permeability at S_{wi} is measured and taken as reference.
To investigate the importance of the effects previously discussed, water imbibition is performed at reservoir rate under multi-rate procedure. After oil production has stopped and differential pressure stabilised, water injection rate is bumped to 80, 160 and 320 cc/h.
Figure 6 displays the oil production and the differential pressure. Graphically, we can observe the early water breakthrough occurs at 0.31 PVinj. The oil production carries on its rising after water breakthrough (at BT only 29.8 % oil recovered) and even more significant output when the pressure gradient is increased. This behaviour is common for an oil-wet sample where the differential pressure overtakes capillary forces and eases the oil release. Additional oil production may also come from smoothing the capillary end effects: a laboratory artefact. For this reason, in-situ saturation monitoring gives valuable information in the interpretation of such flooding tests with heterogeneous rocks.
The in-situ water saturation profiles (Figure 7) display local heterogeneity variation and a possible wettability influence. Capillary end effects are present at the core outlet where capillary pressure is nil. Different saturation profiles have a rather flat aspect, this marks that the early water breakthrough could come from one high permeability corridor (interconnected grapes of vugs throughout the core cylinder). Backwards, the main front will sweep oil from the matrix and the high permeability system is fed by the micropore structure which explains the continuous oil supply after BT out of the core. This behaviour is distinct to homogeneous rock (vugs not connected) where precisely a piston-like displacement is expected.

Steady State Flow (SS)
The sample was saturated with brine salinity of 150 g/l Eq NaCl and the core water permeability was measured. Initial water saturation was set before to saturate core with toluene and prior to flush it with stock tank oil for restoring wettability. A three weeks ageing period is realised by injecting oil at low flow rate, 2cc/h. Then, lightened synthetic oil (1.3 cp) is used to respect the viscosity ratio between reservoir brine and oil. The density at the outlet core is checked to determine when all non lighted oil is fully replaced. Ultimately, the effective oil permeability at S_{wi} is measured and taken as reference.
To investigate the relative permeability at low and intermediate water saturation, water imbibition is performed by applying a constant flow rate (80cc/h). After the oil production and the differential pressure reach a steady trend, fractional water flow is increased stepwise. Eventually, the global water rate is brought to 120, 240 and 320 cc/h. The oil production and the differential pressure are plotted in Figure 9. The in-situ saturation profiles are gathered in Figure 8. No flat water saturation profiles, fluctuations along the core, indicate the need to interpret such experiments taking into account those effects associated with end effects.

The water fractional flow gives indication of the time of water breakthrough. From Figure 10 one infers an early water encroachment for USS method which may traduce unfavourable viscosity ratio or heterogeneity effect. The viscosity effect [7] is discarded according to the magnitude of the viscosity ratio (M= 1.4). The pore layout effect is further investigated with scanner imaging and fluids displacement simulation.
Looking at fluids distribution within core sample gives an interesting approach of the test suitability and strengthens the validity of Steady State flow although a different way to represent field conditions. In one comparative graph (Figure 11), one sees a consistent water saturation front between both methods at different fractional flows. A slight difference in saturation is caused by different capillary end effects as capillary number for USS was 4.1e-07 and 1.8e-06 for SS case at initial conditions.

VISUALISATION OF SMALL-SCALE HETEROGENEITY

The small scale heterogeneity – vugs and carbonate matrix - of the core was characterised by CT scan images.

Porosity Map
The 3D-distribution of the porosity [5] within the core, which represents the static heterogeneity, was the first step of the study. To characterize the pore network, the core was scanned under 2 different states: dry and fully saturated with brine. The differential CT number images represent the presence of brine in the core and so the heterogeneous porous system with a difference of intensity between zones of high and low porosity (see Figure 12a). By using a linear function of porosity versus intensity, this differential CT number image was calibrated. Due to the scanner resolution (512x512 pixels for a transverse section and 1 section every 2 mm), each pixel represents an area of 200µm x 200µm which is bigger than the vugs size. Therefore, a pixel cannot represent a pore and the maximum porosity of a pixel cannot reach 100%.

Two extreme limits of the porosity were fixed at 0% and 45%. The values of the pixels corresponding to both values of porosity were then computed – arithmetic average on the core - to obtain the average porosity measured experimentally. However, to run 3D flow simulation, this CT scan porosity map was then transferred into a regular grid with cell dimensions of 2 x 2 x 2 mm using an arithmetic average of the pixels contained in each cell. It gives us the 3D spacial porosity distribution as depicted on Figure 12b, representative of the CT scan.

Permeability Map

A miscible displacement experiment was performed under CT scan and gives the effluent dispersion curve shown in Figure 5, characterising the dynamic heterogeneity due to the contrast of permeability within the core. Pictures of the miscible displacement experiment at different pore volumes injected (Figure 14) show the fingering of the water front due to the mechanical displacement, which was also observed in 2-phase flow. The accumulation of tracer (Barium Chloride) on the injection face is probably due to a chemical phenomenon. The CT scan permeability map [6] is derived from the CT scan porosity map and based on a porosity-permeability correlation. It was then transferred into the simulation grid using an arithmetic average. To match this permeability upon the experimental one, 3D waterflood simulations were run and the permeability was then corrected. With the final 3D CT scan permeability map, a miscible displacement simulation was performed. The effluent dispersion curve obtained shows clearly the heterogeneity of our model. The calibration process is described with a flow chart in Figure 13.

SIMULATION

Modelling the reservoir performance properly requires the use of correct relative permeability and capillary pressure.

Unsteady State Flow (USS)

The conventional numerical simulation used for relative permeabilities determination is based on a convenient 1D homogeneous model, filled with experimental porosity and absolute permeability. This homogeneous model cannot deal with longitudinal heterogeneities creating early water breakthrough owed to high permeability corridors along the core. Accordingly, mobility ratio has to be forced to unreal level leading to anomalous relative permeability curve shapes and thus not representative of the bulk core properties (Figure 19). So, even if oil throughput, differential pressure and saturation profiles (see Figure 7) seem to match correctly experimental data, the artificial distortion of the relative permeability curves is questionable. Therefore, a fine gridded 3D-model was built instead in a viewpoint to separate geological (static) model from dynamic one, expressed by relative permeabilities, and to enhance core experiments interpretation.

<u>3D – 1 Facies</u>

A first 3D model (see above section) was run by considering the whole core as one facies, bearing the previously determined relative permeabilities, to interpret USS 2-phase flow

experiment. The interpretation of this simulation, with a good match on the fluid productions and differential pressure and with similar saturation profiles, leads to the same relative permeability curve deformation as in the homogeneous case. Moreover, as we can see on the simulation pictures at different time steps (Figure 15), the fingering observed experimentally is not represented with this model. Obviously, the continuous permeability-porosity model used does not efficiently represent the contrast between the vugs and the matrix, even if the simulation of the miscible displacement seemed to overestimate it.

3D – 2 Facies

To model the contrast between the vugs and the matrix, a 2-facies model based on 2 different sets of relative permeability curves for each sub-system was built keeping the same porosity and permeability distribution. The first step was to determine the cells of the model that represent the vug system. Mercury injection enables to determine 2 main facies in the core and the pore volume associated with the vugs (largest pores). Actually, the most porous cells of the model were considered to represent the vug system, until reaching the right pore volume associated, which gives an inferior limit of 34%. The irreducible water saturations in both systems were different: 2% in vugs and 6.71% in matrix to match the initial water volume in the core. Upon the same approach, the residual oil saturation was estimate to 5% in vugs, low value owing to very good sweep efficiency, against 45% in the matrix. Cross-like and Corey type curves were used as input for relative permeability to respectively model flow in the vugs and in the matrix. Although the capillary pressure in the vugs was fixed at 0, a particular attention was focused on the matrix capillary pressure curve to avoid too large spontaneous water imbibition in the matrix; the capillary pressure must be lower than the capillary pressure in the vugs. The final interpretation of the unsteady-state experiment leads to smooth relative permeability curves shown on Figure 19 with a fairly good match of the oil production and the differential pressure (Figure 17).
The match of the in-situ saturations is significantly better showing the importance of the in-situ saturation data as additional constraint on the interpretation (Figure 18). The profiles are less continuous than in the 1-facies model. It can be explained by the strong heterogeneity in saturation in the core which depends directly on the definition of the 2 facies and Z-axis selection. Reversely, the 2-facies model well represents the flow fingering (Figure 16) in vugs and is closer from the experimental observations than the 1-facies model.

Steady State Flow (SS)

The conventional numerical simulation used for relative permeabilities determination is based on a 1D homogeneous model, filled with the experimental porosity and absolute permeability. This model construction does include capillary forces that are occurring in the steady state flow test at initial conditions (see Figure 8). With this model oil production, differential pressure and saturation profiles (see Figure 9) mirror fairly well the experimental data. As previously done, the same fine gridded 3D-model was taken to interpret this permanent flow displacement to improve the core experiments interpretation.

3D – 1 Facies

The first 3D model run was an homogeneous one which gave, as expected, the same results as the 1D homogeneous model. With the 3D porosity and permeability distribution determined above, a 2-phase flow simulation was performed with the same 1D relative permeability curves for the entire model, considering the whole core as one facies. The interpretation of this simulation, with a good match on the fluid productions and differential pressure and with similar saturation profiles, brings no modification of the relative permeability curves since less incline to small scale heterogeneity disturbances.

3D – 2 Facies

To improve the in-situ water saturation profiles and visualise where the residual oil saturation is held, the 2-facies model is reused. 1D interpretation relative permeabilities are inserted for the matrix and cross-like relative permeabilities are set for vugs. The irreducible water saturations in both systems are still different: 2% in vugs and 7.7% in matrix to match the initial water volume in the core. As previously visited, the residual oil saturation was estimate to 5% in vugs, low value owing to very good sweep efficiency, against 45% in the matrix. Although the capillary pressure in the vugs was fixed at 0, a particular attention was focused on the matrix capillary pressure curve which must be different from one measured since not downsized to vugs – matrix cells dimension. The final interpretation of the steady-state experiment leads to smooth relative permeability curves shown on Figure 19 with a fairly good match of the oil production and the differential pressure.

If the saturation profiles keep the same trend and are still similar to the experimental data, the profiles are less continuous than in the 1D homogeneous model and it can be asked do we really have an homogeneous fluid distribution within such heterogeneous carbonates where permeability contrasts offer a different oil trapping.

CONCLUSIONS

The above results give an alternative to interpret or reinterpret laboratory waterflood historical performed under multi-rate flow experiments. The technique has provided meaningful relative permeability curves for heterogeneous carbonates, where the 1D homogeneous model leads to poor definition of relative permeability.

A 3D fine gridded model offers the possibility to discard the small scale heterogeneity effect over the relative permeability measurements. In addition, the fluid saturation distribution through CT scan imagery favours the understanding how the water sweeps out within the porous media at the millimetre scale.

Flooding techniques have to be addressed according to the level of heterogeneity as early as possible to avoid distorted relative permeability curves. The steady state technique have to be used carefully with in-situ saturation monitoring to discriminate between capillary pressure and relative permeability effects since flat homogeneous saturation profiles are not conform in such carbonate rocks.

ACKNOWLEGEMENTS

We thank R. Brugidou, S. Bouzida for the experimental work; S. Guillon and N. Keskes for their assistance with image analyses. We are also grateful to the management of Total for permission to publish this study.

REFERENCES

1. Hamon G., Roy C., “Influence of Heterogeneity, Wettability and Coreflood design on Relative Permeability curves”, SCA 2000-23, 2000, Abu Dhabi (UAE).
2. Kamath J., Meyer R.F., Nakagawa F.M., “Understanding Waterflood Residual Oil Saturation of Four Carbonate Rock Types”, SPE-71505, 2001, New Orleans (Louisiana).
3. Archer J.S., Wong S.W., “Use of a Reservoir Simulator to Interpret Laboratory Waterflood data”, SPE-3351, SPE-AIME 1971, New Orleans (Louisiana).
4. Narayanan K., Deans H.A., “A Flow Model Based on the Structure of Heterogeneous Porous Media”, SPE-18328, 1988, Houston (Texas).
5. Withjack E.M., “Computed Tomography for Rock-Property Determination and Fluid-Flow Visualisation”, SPE-16951, 1987, Dallas (Texas).
6. Withjack E.M., S.K. Graham and C.T. Yang “CT Determination of Heterogeneities and Miscible Displacement Characteristics”, SPE Formation Evaluation, December 1991.
7. Moctezuma-Berthier A., Fleury M., “Permeability Mapping on Vuggy Core sample using Tracer Experiments and Stream-Line Simulations”, SCA-9919, 1999, Golden (Colorado).

setup		Units	#1 USS	#2 SS
Air permeability	*Kg*	[mD]	957	911
Brine permeability	*Kw*	[mD]	947	901
Oil permeability	*Ko(Swi)*	[mD]	807	791
Water permeability	*Kw(Sor)*	[mD]	537	428
Porosity		[%]	27.2	26.3
Pore volume	*PV*	[cc]	132.9	129.9
Connate water saturation	*Swi*	[%]	5.8	7.4
Residual oil saturation	*Sor*	[%]	38.2	30.6

Table 1: Core properties and Waterflood results

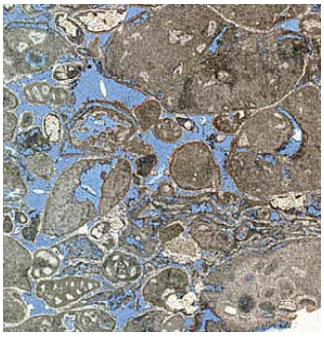

Figure 1: Thin section

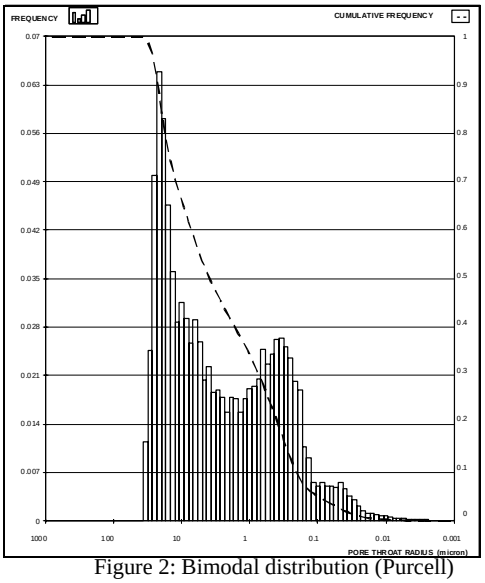

Figure 2: Bimodal distribution (Purcell)

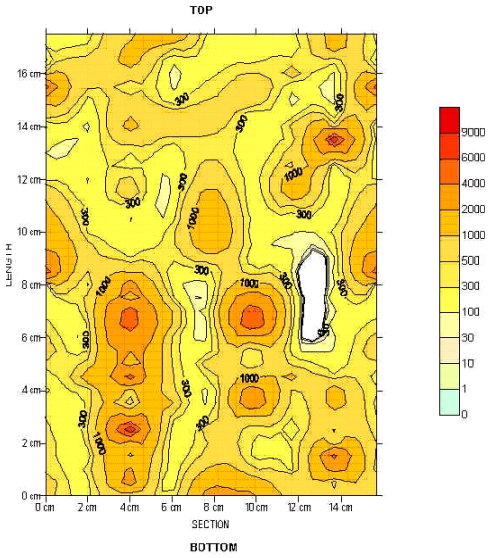

Figure 3: Permeability surface map (Miniperm)

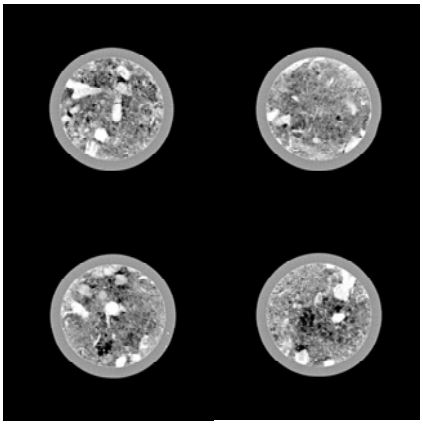

Figure 4: Tomographic images (CT scan)

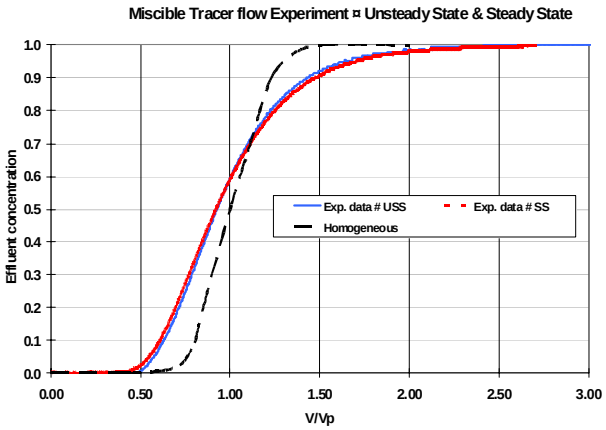

Figure 5: Brine/Brine tracer test before each flow displacement

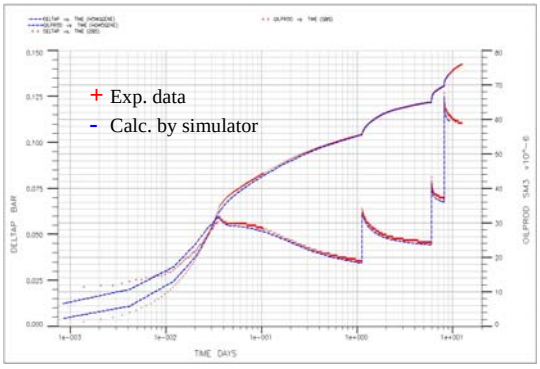

Figure 6: Oil production & Differential pressure (USS, 1D model)

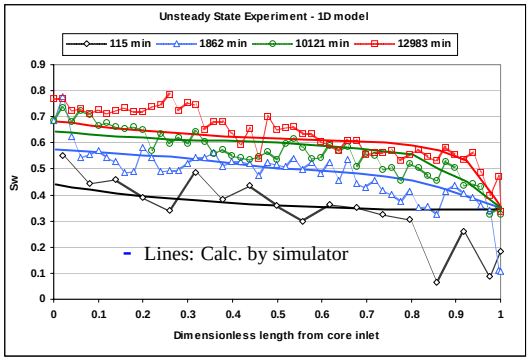

Figure 7: In-situ water saturation profiles (USS, 1D model)

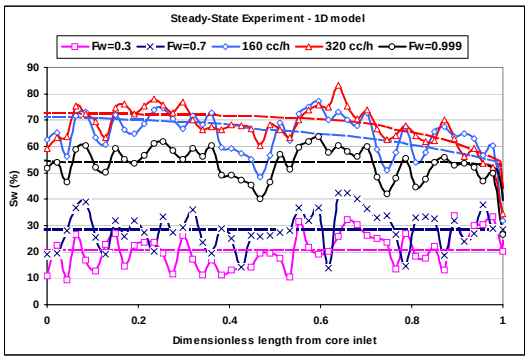

Figure 8: In-situ water saturation profiles (SS, 1D model)

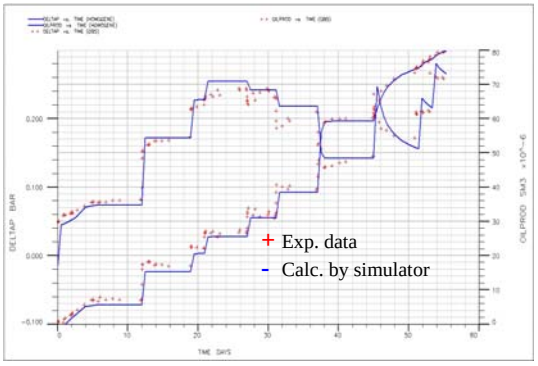

Figure 9: Oil production & Differential pressure (SS, 1D model)

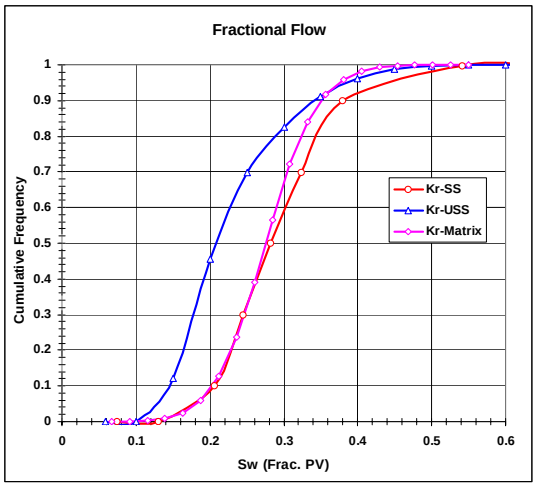

Figure 10: Fractional flow for USS and SS

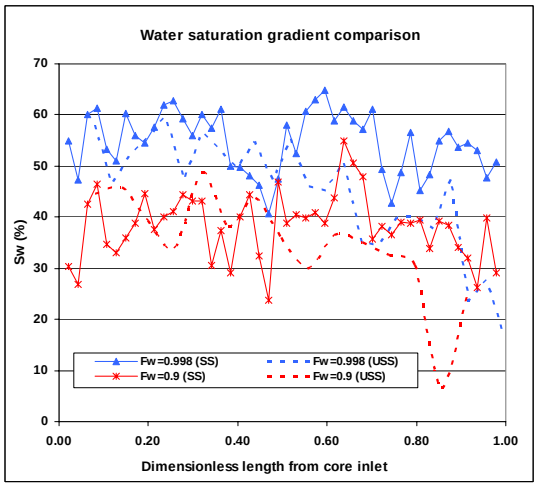

Figure 11: Comparison of Sw profiles data

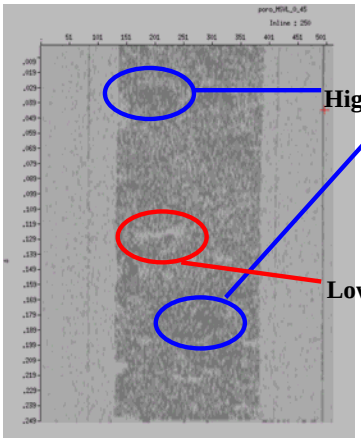

Figure 12a: CT scan porosity map

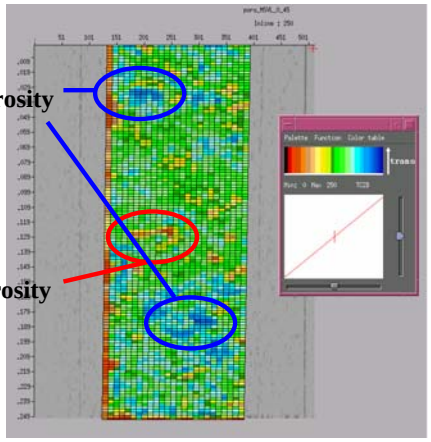

Figure 12b: 3D fine gridded porosity map

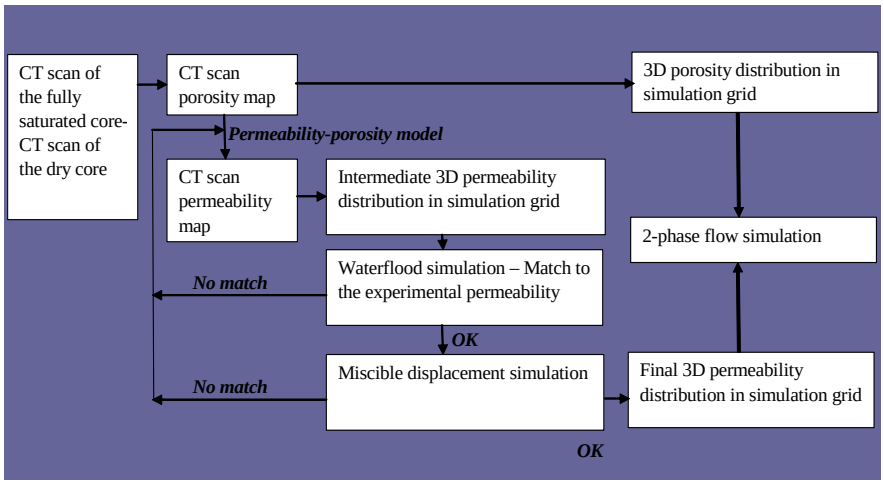

Figure 13: Flow chart for calibration process

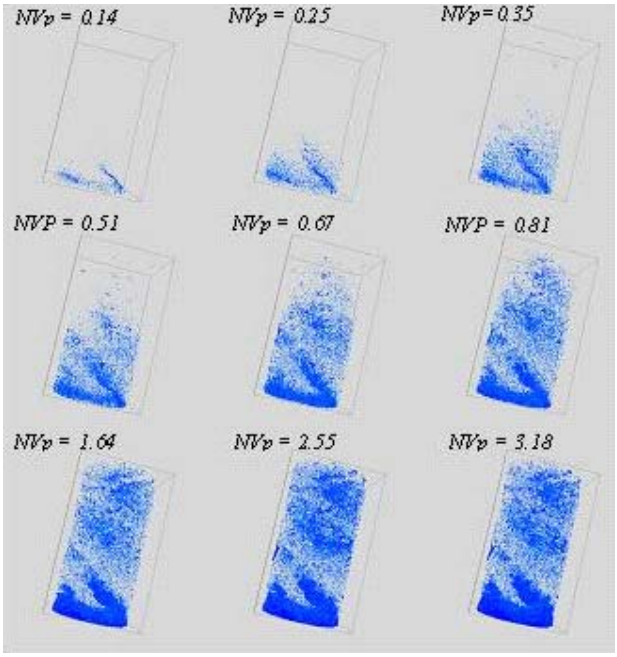

Figure 14: Miscible displacement experiment under CT scan

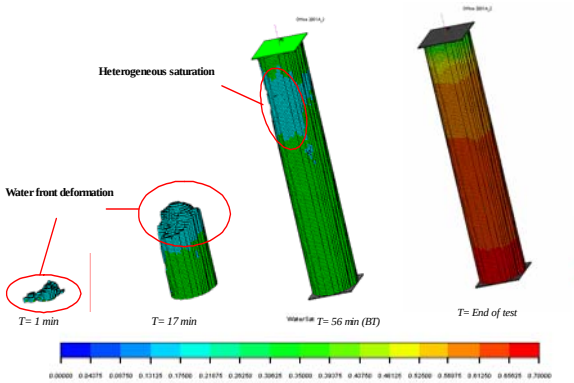

Figure 15: Water saturation front for 1Facies model (USS)

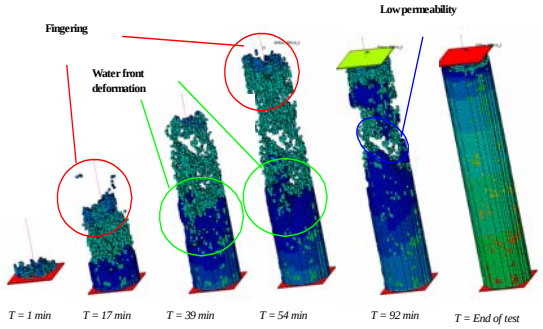

Figure 16: Water saturation front for 2Facies model (USS)

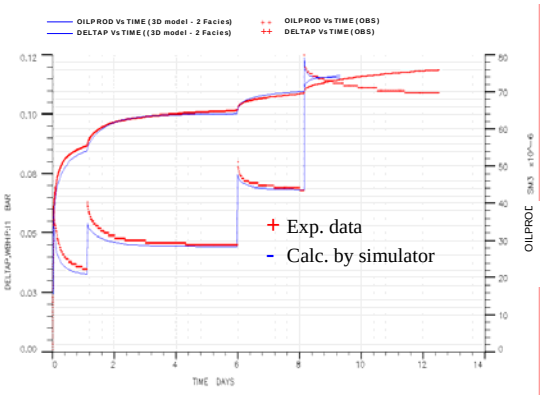

Figure 17: History match of oil production & DP (2Facies)

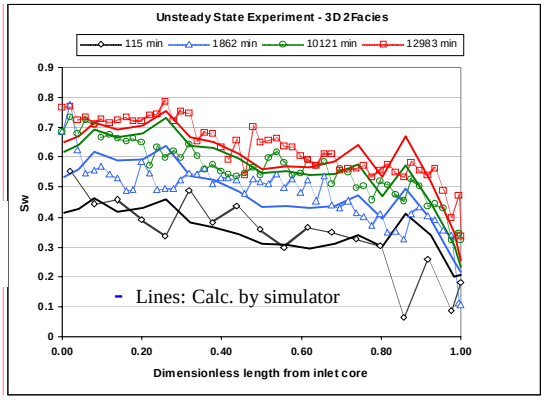

Figure 18: In-situ water saturation profiles (USS, 3D-2 Facies model)

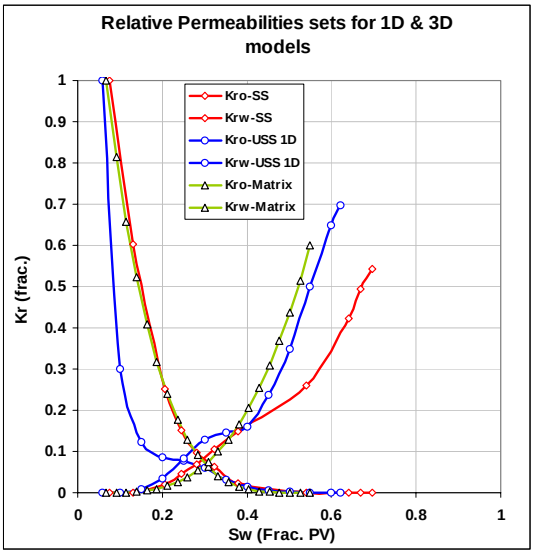

Figure 19: Relative permeability sets (USS, SS, Matrix)

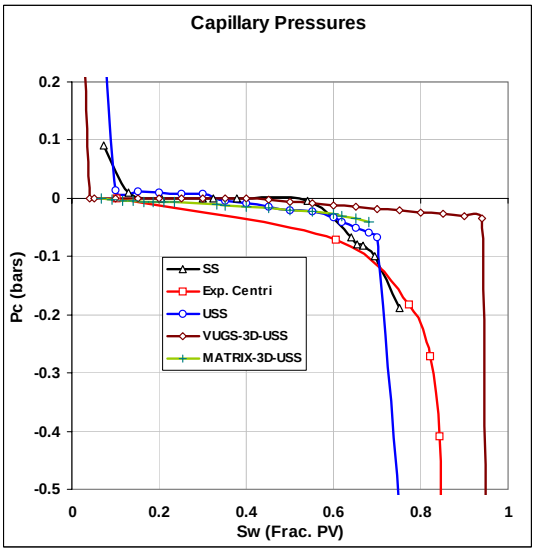

Figure 20: Capillary Pressure curves